

Application of soft x-ray lasers

S Hatae* and G J Tallents

Department of Physics

University of York

York YO10 5DD

United Kingdom

*Permanent address: Nano-physics Division

First Patent Examination Department

Japan Patent Office

3-4-3, Kasumigaseki, Chiyoda-ku, Tokyo, 100-8915, JAPAN

Email: hatae-susumu@jpo.go.jp

Abstract

This paper seeks to review published applications of soft x-ray lasers that have been demonstrated. They include applications using interference such as interferometry and holography, applications using absorption such as microscopy and radiography, and other applications such as Thomson scattering and nonlinear optics. Suggested applications for x-ray free electron lasers are also introduced.

1. Introduction

Since the first demonstration of a soft x-ray laser by Matthews et al in 1985 [1], efforts to improve the features of soft x-ray lasers, such as the brightness, pulse duration, temporal and spatial coherence, spectral bandwidth and collimation, have been made. There are now several reviews of soft x-ray lasers [2, 3]. To date a soft x-ray laser at the shortest wavelength of 5.9 nm with saturated output has been obtained by using electron collisional pumping in a laser-produced plasma as the gain medium [4]. Some applications of soft x-ray lasers utilizing these features have been demonstrated and this paper seeks to review published applications.

Applications using interference (i.e. the real part of the index of refraction) including interferometry, holography and deflectometry are first introduced. Applications using absorption (i.e. the imaginary part of the index of refraction) including microscopy and radiography are then discussed. Other applications such as Thomson scattering and nonlinear optics are subsequently surveyed.

Several x-ray free electron lasers are under construction [33, 34, 35, 36], Suggested applications of these free electron lasers that may be applicable to plasma-based soft x-ray lasers are considered.

2. Interferometry

Soft x-ray laser interferometry can be used for measurements in material science, metrology and especially dense plasma diagnosis. Two types of soft x-ray laser interferometry have been applied in practice. Amplitude division interferometry (for example, using a Mach-Zehnder interferometer [5]) and wavefront division interferometry (for example, using a Fresnel double-mirror [6] or Lloyd's mirror [7, 8]) have been employed. Amplitude division interferometry requires high temporal coherence, while wavefront division interferometry requires high transverse coherence.

The first soft x-ray laser interferometry was demonstrated by DaSilva et al in 1995 [5]. In this first demonstration, an amplitude division type Mach-Zehnder interferometer consisting of two multilayer beam splitters and two multilayer mirrors was used as shown in figure 2-1. In measurements of electron density in plasmas by interferometer, the number of fringe shifts, N_{fringe} , is related to the electron density n_e by

$$n_{cr} = \frac{1.1 \times 10^{21}}{\lambda^2 (\mu m^2)} (cm^{-3}) \quad (1)$$

$$N = \sqrt{1 - \frac{n_e}{n_{cr}}} \quad (2)$$

$$N_{fringe} = \frac{1}{\lambda} \int_0^L (1 - N) dl \approx \frac{n_e L}{2n_{cr} \lambda} \quad (3)$$

where n_{cr} is the critical electron density for the soft x-ray laser, N is the index of refraction and L is the plasma length along the probe beam path. A high density laser-produced CH plasma of long length (≈ 0.7 mm) was probed by a soft x-ray laser at a wavelength of 15.5 nm from laser-produced Neon-like yttrium lasing and the electron densities of the plasma (up to $n_e \approx 10^{21} \text{ cm}^{-3}$) were successfully measured by DaSilva et al.

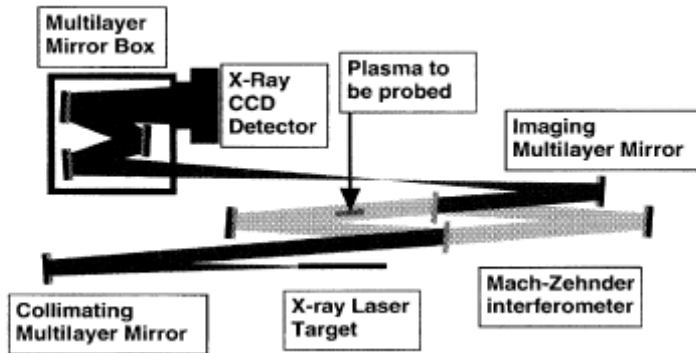


Figure 2-1: Experimental setup of soft x-ray laser interferometry by DaSilva et al [5]

As demonstrated by DaSilva et al, soft x-ray laser interferometry is especially useful for probing large, high density and expanding plasmas. The short duration of the probe pulse is desirable to obtain the electron density profile of the fast evolving plasma by reducing the effects of plasma motion blurring. In addition, shorter wavelength lasers compared with optical or UV lasers minimize effects associated with refraction and free-free absorption. In optical laser interferometry, the size of the plasma and the peak electron density accessible are severely restricted by these effects.

Characteristics of multilayer beam splitters used in the first demonstration above are dependent on the wavelength of soft x-ray lasers. Though multilayer mirrors had been obtained for a wide range of wavelength, multilayer beam splitters with both appropriate reflectivity and transmittance for various wavelengths were not easy to obtain. This restricts the available wavelength suitable for multilayer beam splitters. Other types of soft x-ray lasers interferometry without multilayer beam splitters have consequently been developed to eliminate the need for wavelength dependent optics.

One solution is wavefront division interferometry. The first demonstration of soft x-ray lasers using wavefront division interferometry was done by Albert et al in 1997 [6]. A Fresnel double-mirror was used in this demonstration as shown in figure 2-2 and the interferogram from a silica substrate sample with a step was obtained. Another type of wavefront division interferometry which uses a Lloyd's mirror was first demonstrated by Rocca and Moreno et al in 1999 [7, 8]. Their experimental setup is shown in figure 2-3. In this demonstration, a capillary discharge pumped soft x-ray laser at wavelength of 46.9nm was used to obtain the electron density profile of a pinch plasma.

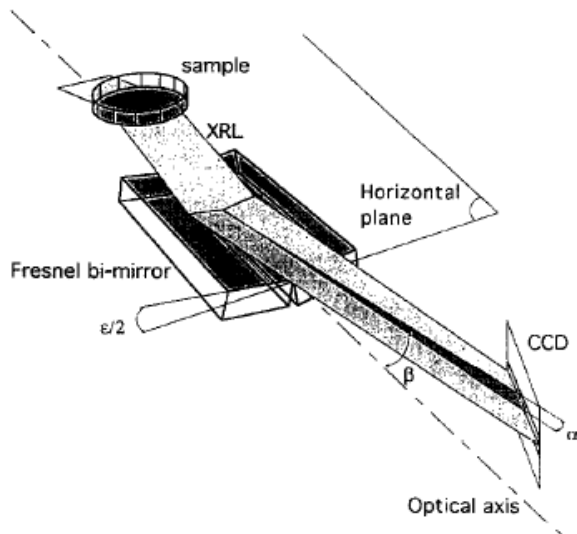


Figure 2-2: Fresnel double-mirror interferometer by Albert et al [6]

Another solution is using diffraction gratings instead of multilayers as beam splitters for amplitude division type interferometer. Filevich et al demonstrated soft x-ray laser Mach-Zehnder interferometry using diffraction gratings as beam splitters in 2000 [9].

As mentioned above, plasmas have often been probed by soft x-ray laser interferometer in initial demonstrator experiments. However, the probing of other targets has also been undertaken. Zeitoun and Zeitoun-Fakiris et al observed Nb surface deformation under high electric fields by soft x-ray laser interferometry with a Fresnel double mirror [10, 11].

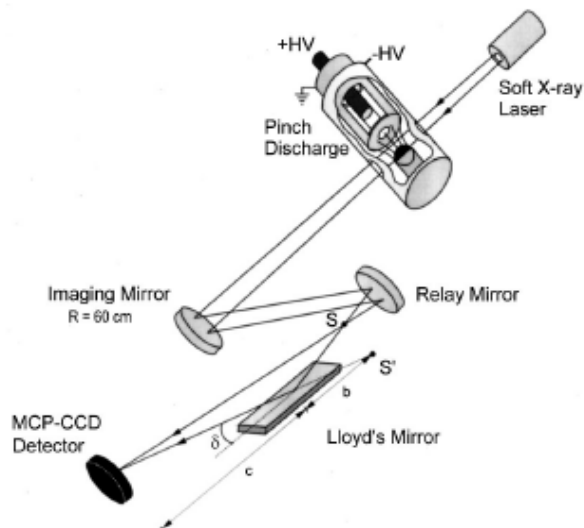


Figure 2-3: Lloyd's mirror interferometer by Moreno et al [8]

Recently, Filevich et al observed the index of refraction of plasma greater than one using an x-ray laser interferometry [12]. Previously, the index of refraction had been determined by the free electrons density and the contribution of the free electrons to the index of refraction was always less than one. Filevich et al suggested a contribution to the index of refraction from bound electrons that is expressed by

$$N = \sqrt{1 - \sum_z \frac{n_z f_z^*}{n_{cr}}} \quad (4)$$

where n_z is the density of ions with charge Z and f_z^* is the sum of the separate contributions of free and bound electrons. A value of f_z^* can be negative because the component of the contribution of bound electrons is negative. Therefore, the index of refraction can be greater than one. Fringe shifts indicating an index of refraction greater than one were observed in soft x-ray laser interferograms of a laser-produced Al plasma by an amplitude division diffraction grating interferometer with a Ni-like Pd soft x-ray laser operating at a wavelength of 14.7nm.

3. Holography

Soft x-ray laser holography offers the potential to obtain high-resolution three-dimensional images of biological and other specimens. High-resolution images can be obtained because of the high coherence and the high brightness of soft x-ray lasers that enables a single shot record. Exposure times can be reduced to < 1 nsec, which eliminates motion blurring in biological samples as the dynamic processes in biology have time scales of typically 1 msec. Synchrotron x-ray holography and undulator x-ray holography typically needs 1 to 1000 sec exposure times from many shots.

The first demonstration of soft x-ray laser holography was carried out by Trebes et al in 1987 [13]. A Gabor in-line type holography geometry with a high reflectivity multilayer mirror as a narrow bandpass filter was employed in this demonstration as shown in figure 3-1. Without the multilayer mirror, the continuum emission from a plasma as a laser amplifier would reduce the fringe visibility in the hologram. The object beam resulting from the x-rays scattered forward by object, and the reference beam resulting from the x-rays missing the object, interfere and produce a hologram at the detector. The hologram of a three dimensional structure of a gold test pattern was recorded by using the Ne-like Se soft x-ray laser with a wavelength of 20.6 nm and pulse length of 200 psec. The image was reconstructed by illuminating with a

helium-neon laser with resolution of 2-3 μm .

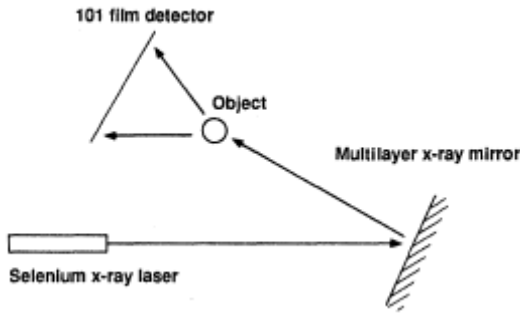


Figure 3-1: Experimental setup of soft x-ray laser holography by Trebes et al [13]

The optimal wavelength of soft x-ray laser holography for observing wet biological samples was discussed by London et al in 1989 [14]. In this discussion, the dose absorbed by the sample should be minimized for given x-ray laser fluence so that sufficient scattered photons to enable the production of a hologram are produced. According to the results, a wavelength of slightly longer than the 4.37 nm carbon K-edge is best for minimizing the necessary source power and the dose absorbed by sample.

4. Deflectometry

Soft x-ray laser deflectometry has also been utilized to probe laser-produced plasmas. The short wavelength results in only a small amount of refraction and this allows the measurement of higher electron densities of larger plasmas. The short pulse duration is preferable for observing the rapid evolution of the plasma.

Ress et al measured the electron density of laser-produced plasma with a Ne-like Y soft x-ray laser ($\lambda=15.5$ nm) Moiré deflectometer in 1994 [15]. The experimental setup is shown in figure 4-1. The index of refraction for x-ray lasers thorough a probed plasma is given by equation (2). Considering a soft x-ray laser travelling thorough a plasma along the target surface, and assuming the plasma density varies only in the direction normal to the target surface (say, the x-direction), the bending angle ϕ of the soft x-ray laser is given by

$$\phi = \int_{-\infty}^{S_0} \frac{dN}{dx} ds = -\frac{1}{2n_c} \int_{-\infty}^{S_0} \frac{\partial n_e}{\partial x} ds \quad (5)$$

assuming $n_e \ll n_c$. The value of ϕ can be measured by Moiré deflectometry and the electron density n_e can be solved by the equation above given a proper boundary

condition. The electron density profile of a 3 mm long plasma was obtained with peak density of $3.2 \times 10^{21}/\text{cm}^3$ by Ress et al.

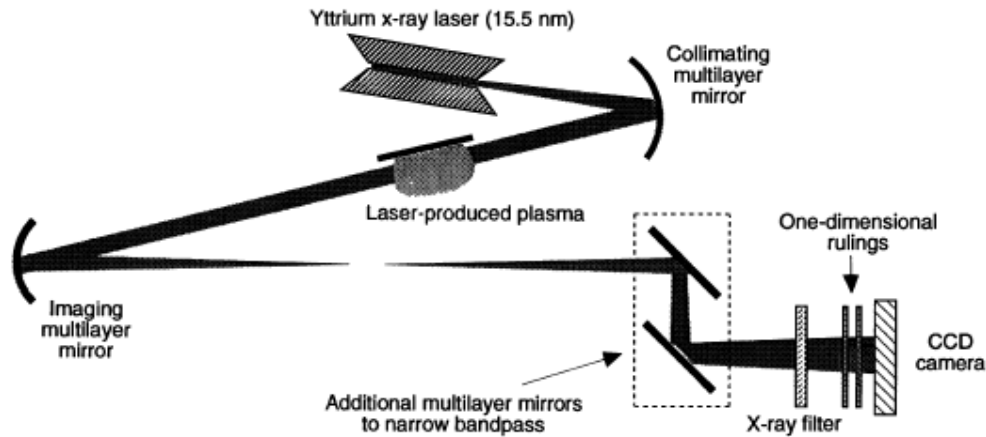


Figure 4-1: Experimental setup of soft x-ray laser deflectometry by Ress et al [15]

5. Microscopy

Soft x-ray laser microscopy offers the opportunity to observe biological specimens in an aqueous environment. A goal here would be to have lasing at wavelengths near or inside the water window (2.3-4.5 nm) where the high contrast in absorption cross section between carbon in biological specimens and oxygen in water can be obtained (see [14]). However, as soft x-ray lasers cannot be routinely produced at wavelengths shorter than ~ 10 nm, other wavelength ranges have been employed for microscopy. The high brightness and short duration of soft x-ray lasers enable the elimination of problems associated with motion blurring and radiation-induced chemical decomposition of biological specimen.

In 1988, Skinner et al carried out the first demonstration of soft x-ray laser microscopy. Images of a piece of wire mesh were recorded on film and on resist with an 18.2 nm wavelength soft x-ray laser using contact microscopy [16]. Suckewer et al produced images of dehydrated cancer cells on photoresist by composite optical / x-ray laser contact microscopy (shown in figure 5-1) in 1990 [17].

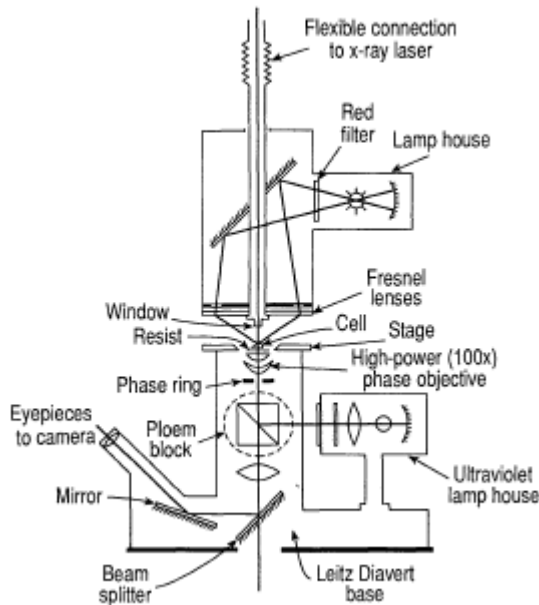


Figure 5-1: Composite optical / soft x-ray laser contact microscopy by Suckewer et al [17]

DaSilva et al demonstrated soft x-ray laser microscopy using a Fresnel zone plate lens and imaged a test pattern with resolution of 75 nm with a Ni-like Ta soft x-ray lasers at a wavelength of 4.483 nm in 1992 as shown in figure 5-2 [18]. Rat sperm nuclei were also observed in a subsequent demonstration in 1992 [19]. The soft x-ray laser had energy of 10 μ J in 400 ps. In this demonstration soft x-ray laser microscopy could resolve structures of size of about 50 nm.

Since then, not many demonstrations of soft x-ray laser microscopy have been reported. One reason is that no saturated soft x-ray laser at wavelengths inside the water window (2.3-4.4 nm) has been achieved. In addition, the coherence characteristics of soft x-ray lasers are not beneficial for microscopy because of the problem of fringes or speckle. In order to stimulate the development of soft x-ray laser microscopy, soft x-ray laser saturation at a wavelength in the water window is probably required.

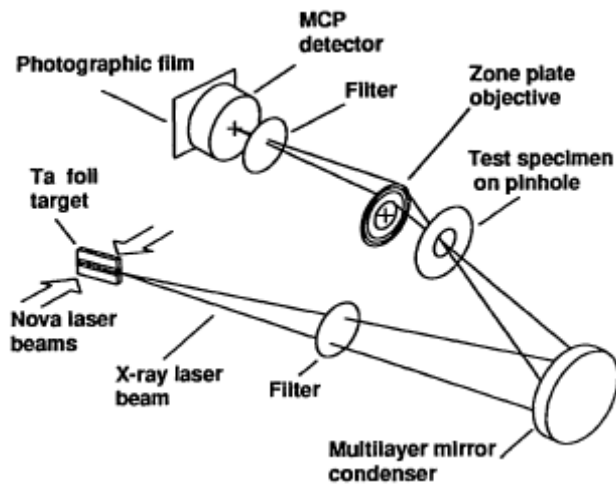


Figure 5-2: Experimental setup of soft x-ray laser microscopy by DaSilva et al [19]

6. Radiography

Soft x-ray laser radiography is useful for measuring plasma parameters. The short pulse duration (3-500 ps) of soft x-ray laser is of the same scale as the hydrodynamic timescale of laser-produced plasma. The high brightness of soft x-ray lasers allows them use as a backlighter for the imaging of bright sources such as high temperature plasmas. The short wavelength enables the x-ray laser to probe larger and higher density plasmas.

Cauble et al observed laser-accelerated foils by soft x-ray laser radiography in 1995 [20]. A Ne-like Y soft x-ray laser at a wavelength of 15.5 nm probed the foils from the direction parallel to the target surface (side-on) and small-scale breakup of the foils due to laser imprint was observed. Their experimental setup is illustrated in figure 6-1. X-ray heated foils were also probed and near-volumetric heating with slight asymmetry between front side and rear side was observed.

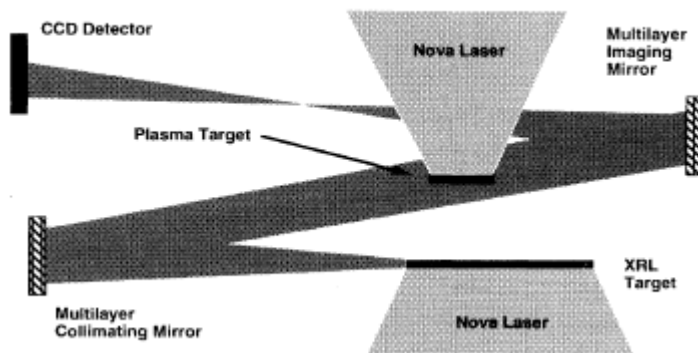


Figure 6-1: Experimental setup of side-on soft x-ray laser radiography by Cauble et al

[20]

Measurement of the early laser imprint and subsequent Rayleigh-Taylor instability is of interest especially in studying direct drive inertial confinement fusion. In order to develop measurements of laser imprint, soft x-ray laser face-on radiography was demonstrated by Key et al in 1995 [21]. In this demonstration, a Ne-like Y soft x-ray laser at wavelength of 15.5 nm irradiated the target in a direction perpendicular to target surface and Si foil with etched bar pattern was observed. Kalantar et al utilized this radiography to observe practically as shown in figure 6-2 laser imprinted modulation in a Si foil [22, 23].

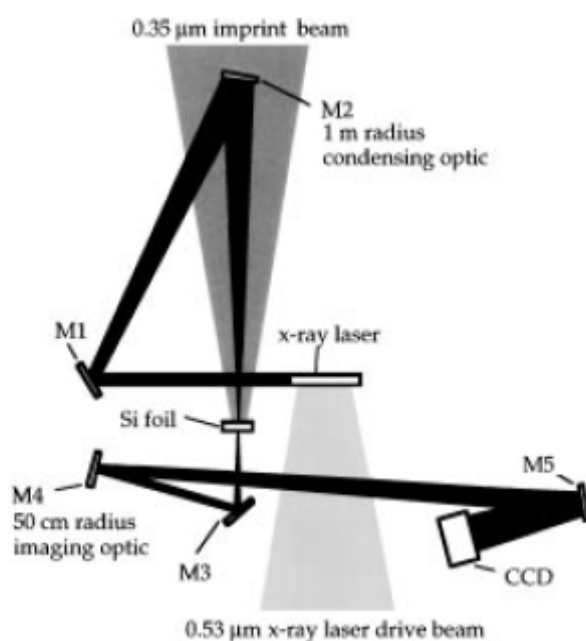


Figure 6-2: Experimental setup of face-on soft x-ray laser radiography by Kalantar et al [23]

Wolfrum et al probed laser irradiated Al foils by soft x-ray laser radiography with a probe laser of Ne-like Ge at a wavelength of 19.6 nm [24]. Temporal development of a single mode laser imprinted modulation including Rayleigh-Taylor growth was measured. The temporal change in opacity of shock compressed Al was also measured with the Ne-like Ge x-ray laser.

7. Thomson scattering

Thomson scattering is an important method to measure densities and temperature of plasmas. X-ray laser Thomson scattering has potential for probing

plasmas at higher density than optical probing, even above the solid density. A laser entering a plasma is scattered by electrons. The temperature of plasma can be measured by observing the spectrum of scattered light and the density of plasma can be measured by observing the amount of scattered light.

An attempt to record x-ray laser Thomson scattering was carried out by Khattak and Riley et al using a Ne-like Ni x-ray laser at a wavelength of 23.1nm [25, 26]. Figure 7-1 shows the experimental arrangement of x-ray laser Thomson scattering by Khattak et al. In the illustrated experimental arrangement, a CH foil was used as a main target and was irradiated to produce uniform plasma by x-rays from two Au foils, which were irradiated by two backlighter beams. The CH foil was directly irradiated by the two backlighter beams in another experimental configuration.

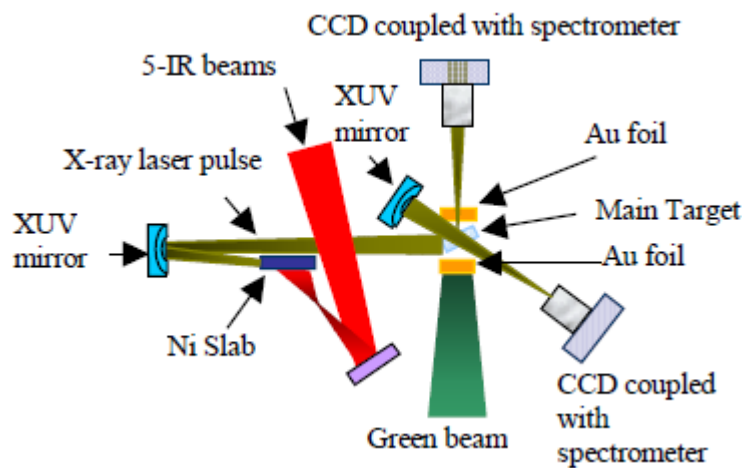


Figure 7-1: Experimental setup of x-ray laser Thomson scattering by Khattak et al [25]

As the Thomson scattering cross-section is very small, it is difficult to gain a signal above the noise level caused by plasma emission. Because of this, soft x-ray laser Thomson scattering experiments have not succeeded in observing scattered spectrum so far. To improve the situation, soft x-ray lasers of higher brightness at a shorter wavelength and/or development of better reflectivity for an x-ray laser mirror are necessary.

8. Nonlinear optics

Nonlinear optics in the soft x-ray region has the potential to extend the operating wavelengths of soft x-ray lasers through harmonic generation, frequency conversion or parametric oscillation. Nonlinear optics processes would also allow the measurement of soft x-ray laser pulses shapes and widths with a high temporal

accuracy by cross- and auto-correlation.

Muendel et al discussed the feasibility of a four-wave sum-difference-frequency generation in soft x-ray region [27]. As conventional solid, liquid and gaseous media for optical wavelength are unsuitable as a nonlinear medium for the soft x-ray region due to the strong absorption, highly stripped ions in a plasma were suggested as a nonlinear medium. Nonlinear susceptibilities and converted intensities as a function of incident frequencies were calculated for the specific plasma as a nonlinear medium. Topping et al carried out experiments of a four-wave sum-difference-frequency generation using two x-ray lasers at 23.1 nm from Ne-like Ni and one optical laser at 1.054 μm as incident waves and a Na-like Ar plasma as a nonlinear medium [28].

Harmonic generation, frequency conversion and parametric oscillation in the soft x-ray region have not succeeded yet probably because of a lack of detailed knowledge of the spatial coherence properties of x-ray lasers.

Nabekawa et al observed doubly charged helium ions produced by the two-photon double ionization of helium atoms using 42eV photons of the 27th harmonic of a Ti: sapphire laser [29]. In this experiment, the yields of singly charged helium ions and doubly charged helium ions were measured as in Figure 8-1. The yield of singly charged ions was assumed to be proportional to the intensity of the 27th harmonic. The experimental results show that the yield of the doubly charged ions depends quadratically on the yield of singly charged ions, and therefore on the intensity of the 27th harmonics. This indicates the production of the doubly charged helium ions are due to the two-photon absorption with double ionization. Nabekawa et al also successfully measured a pulse duration of the 27th harmonic pulse of 8 fs by an autocorrelation technique using the two-photon absorption process.

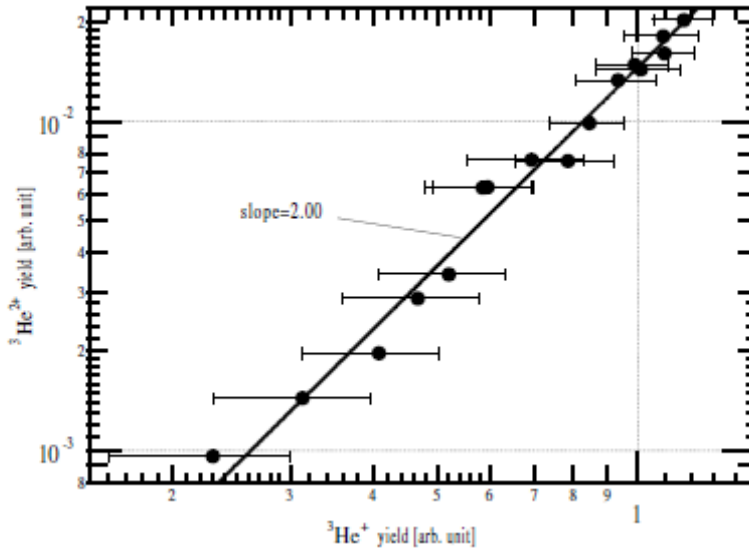


Figure 8-1: Relationship between the yield of the doubly charged helium ions and the yield of the singly charged helium ions by Nabekawa et al [29]

9. Other applications

Tomassetti et al produced photoluminescent patterns of colour centres in crystals by irradiating with soft x-ray lasers of 46.9 nm produced in capillary discharge [30]. Soft x-ray lasers can carry out colouration in shorter exposure times with better spatial resolution compared to conventional methods such as x-ray radiation and electron beam implantation. Interferometric patterns generated by soft x-ray lasers reflected by a Lloyd's mirror were utilized to produce periodic linear photoluminescent patterns in the LiF crystals with various spatial resolutions down to 1.2 μm .

Jamelot et al used a soft x-ray laser as an excitation source for luminescence [31]. The narrow spectra bandwidth of a soft x-ray laser realises a high spectra resolution of the emission bands. CsI luminescence in the UV-visible region was excited by a soft x-ray laser at 21.2 nm. The quenching of luminescence was observed as the intensity of the soft x-ray laser increased, possibly due to nonradiative recombination that was caused by the high intensity of the soft x-ray laser.

Tallents et al carried out direct measurements of the opacity of near solid density iron plasmas at temperatures of $\sim 60 - 300$ eV by Ni-like silver soft x-ray lasers at the wavelength of 13.9 nm as the backlighter [32]. Good agreement was obtained between the experimental data and the result of a simulation for early stage of the plasma expansion.

10. Prospective applications

X-ray free electron lasers (XFEL) generated by self-amplified spontaneous emission are under development [33, 34, 35, 36] (see table 1). An XFEL can be expected to have ultra-intense and ultra-short pulses with full transverse coherence, peak power of a few to tens of GW, pulse length of the femtosecond range and tunable photon energy up to several keV photon energy. Average power is also higher than current sources as a pulse repetition rate of 1 kHz is expected. The pulse length durations of these sources (~femtoseconds) correspond to the time scales of atomic motions and the high intensity enables a single short pulse shot to carry out various measurement. Some applications making use of these features have been suggested [35, 37, 38, 39, 40].

Femtochemistry is one of the key applications of an XFEL. Femtochemistry by pump-probe spectroscopy aims at real-time observation of transient molecular behaviours including the atomic positions, bond lengths and angles during chemical reactions. As chemical reactions occur with timescales of order of femtoseconds or picoseconds and structural changes occur on an atomic scale, high spatial and temporal resolution corresponding to these scales are required to observe molecular motion in real time. An XFEL has sufficient spatial and temporal resolution for this purpose. Even for such a short pulse, the photon flux per pulse of an XFEL is still enough to carry out spectroscopic observations with a single pulse. An XFEL can provide an opportunity to observe various nanoscale dynamics spectroscopically, such as viscoelastic flow, protein folding, crystalline phase transitions, and magnetization dynamics of nanostructures over a wide range of time scales.

Structures of biomolecules such as protein with atomic resolution will be determined by x-ray diffraction with an XFEL. The high brightness of the XFEL produces enough scattering to record diffraction pattern of very small samples such as single particles of large macromolecular assemblies without the need for sample to be crystalline where large signals are obtained due to coherent addition of the electric field of the x-rays by Bragg reflection. As pulse lengths of femtosecond range are short enough to avoid image blurring due to the vibrational motion of nuclei, atomic structure can be obtained without averaging over any periodic atomic motions. An XFEL is suitable for observing biological specimens in their natural wet environment. Though radiation damage may be a problem, the very short period of femtosecond scale pulse can be expected to allow the collection of diffraction patterns before radiation damage that distorts or destroys the biomolecule structure occurs. A large degree of spatial coherence of an XFEL is also ideal to record a 3-D image by holographic technique.

Imaging at the atomic scale can be obtained by x-ray microscopy with an XFEL. X-ray microscopy can obtain images of non-crystallised specimens while x-ray diffraction requires samples to have a periodic structure. This enables us to observe amorphous and disordered materials, including polymers, crystals with strains and defects, inorganic structures such as nanotubes, and bio-molecules that are difficult to crystallize.

Some fundamental scientific experiments that have not been able to be carried out so far with other light source such as synchrotron radiation can also be carried out with an XFEL. They include studying of plasma, warm dense matter and atomic physics, e.g. determination of energies, ionization cross sections, lifetimes and transition rates. The high intensity of an XFEL will enable nonlinear effect that leads to multiphoton processes around the keV region.

An XFEL may be as a light source for nanolithography. The high power and short wavelength of XFEL may realize controlled structures in the nanometre range that is still a big challenge for industry.

Facility	LCLS	BESSY	TESLA	MIT Bates	4GLS
Place	Stanford, United States	Berlin, Germany	Hamburg, Germany	Massachus etts, United States	Daresbury, United Kingdom
Wavelength (nm)	1.5-0.15	51-1.24	6.4-0.1	100-0.3	124-12.4
Pulse Duration (fs)	77	20	100	50	10
Peak Brightness (10^{30} **)	64-850	1.6-13	60- 5,400	1,000	35
Average Brightness (10^{20} **)	20-270	0.8-6.8	3,000- 160,000	500	50
Peak Power (GW)	19-8	14-1.5	135-24	4	
Average Power (W)	0.61-0.25	0.260-0.016	800-72	0.2	
Number of photons per pulse (10^{12} Photons/pulse)	27.9-1.1	70-0.2	430-1.2	0.3	70
Peak photon flux (10^{25} Photons/s)	14.5-0.59	16-1		0.6	700
Average photon flux (10^{15} Photons/s)	-0.13	70-0.2	26,000-36	0.3	1000
Beam size (FWHM) (μm)	109-96	160-14	65-110		70
Beam divergence (FWHM) (μrad)	13-1.5	140-37	27-0.8		
Repetition rate (Hz)	120	1,000	10	1,000	1,000

** Photons/(s, mm², mrad², 0.1%BW)

Table 9-1: Summary of parameters for several x-ray and soft x-ray free electron lasers under development

10. Conclusion

Some applications of x-ray lasers have been introduced. They are still under development. As far as a plasma-produced x-ray laser is concerned, realisation of saturation at a shorter wavelength, especially in the water window region, will lead to new applications, for example, x-ray diffraction measurement to determine molecular structures. Plasma-based x-ray lasers have the advantage of a relatively low cost compared to the x-ray free electron lasers currently under development.

References

- [1] Matthew D L, Demonstration of a Soft X-Ray Amplifier, *Physical Review Letters*, 54, 110 (1985)
- [2] Tallents G J, The physics of soft x-ray lasers pumped by electron collisions in laser plasmas, *Journal of Physics D: Applied Physics*, 36, R259 (2003)
- [3] Daido H, Review of soft x-ray laser researches and developments, *Reports on Progress in Physics*, 65, 1513 (2002)
- [4] Smith R, Saturation behaviour of two x-ray lasing transitions in Ni-like Dy, *Physical Review A*, 59, R47 (1999)
- [5] DaSilva L B, Electron Density Measurements of high Density Plasmas Using Soft X-Ray Laser Interferometry, *Physical Review Letters*, 74, 3991 (1995)
- [6] Albert F, Interferograms obtained with a X-ray laser by means of a wavefront division interferometer, *Optics Communication*, 142, 184 (1997)
- [7] Rocca J J, Soft-x-ray laser interferometry of a plasma with a tabletop laser and a Lloyd's mirror, *Optics Letters*, 24, 420 (1999)
- [8] Moreno C H, Soft-x-ray laser interferometry of a pinch discharge using a tabletop laser, *Physical Review E*, 60, 911(1999)
- [9] Filevich J, Dense plasma diagnostics with an amplitude-division soft-x-ray laser interferometer based on diffraction gratings, *Optics Letters*, 25, 356 (2000)
- [10] Zeitoun Ph, Investigation of strong electric-field induced surface phenomena by soft X-UV laser interferometry, *Nuclear Instruments and Methods in Physics Research Section A*, 416, 189 (1998)
- [11] Zeitoun-Fakiris A, Observation by soft X-ray laser interferometry of Nb cathode surface evolution during very high electric field application, *IEEE Transactions on Dielectrics and Electrical Insulation*, 6,418 (1999)
- [12] Filevich J, Observation of a Multiply Ionized Plasma with Index of Refraction Greater than One, *Physical Review Letters*, 94, 035005 (2005)
- [13] Trebes J E, Demonstration of X-ray Holography with an X-ray Laser, *Science*, 238,

517 (1987)

- [14] London R A, Wavelength choice for soft x-ray laser holography of biological samples, *Applied Optics*, 28, 3397 (1989)
- [15] Ress D, Measurement of Laser-Plasma Electron Density with a Soft X-ray Laser Deflectometer, *Science*, 265, 514 (1994)
- [16] Skinner C H, Toward Shorter Wavelength Lasers and Soft X-Ray Laser Microscopy, *IEEE Transaction on Plasma Science*, 23, 134 (1988)
- [17] Suckewer S, Soft X-Ray Lasers and Their Applications, *Science*, 247, 1553 (1990)
- [18] DaSilva L B, Demonstration of X-Ray Microscopy with an X-Ray Laser Operating near the Carbon K Edge, *Optics Letters*, 17, 754 (1992)
- [19] DaSilva L B, X-ray Laser Microscopy of Rat Sperm Nuclei, *Science*, 258, 269 (1992)
- [20] Cauble R, Micron-Resolution Radiography of Laser-Accelerated and X-Ray Heated Foils with an X-Ray Laser, *Physical Review Letters*, 74, 3816 (1995)
- [21] Key M H, New plasma diagnostic possibilities from radiography with x.u.v. lasers, *Journal of Quantitative Spectroscopy and Radiative Transfer*, 54, 221 (1995)
- [22] Kalantar D H, X-ray laser radiography of perturbations due to imprint of laser speckle in 0.35 μm laser irradiation of a thin Si foil, *Review of Scientific Instruments*, 67, 781(1996)
- [23] Kalantar D H, Measurement of 0.35 μm laser imprint in a thin Si foil using an x-ray laser backlighter, *Physical Review Letters*, 76, 3574 (1996)
- [24] Wolfrum E, X-UV laser radiography, *Comptes rendus de l'Academie des sciences Serie IV Physique, astrophysique*, 1, 1105 (2000)
- [25] Khattak F Y, X-ray laser Thomson Scattering, *Central Laser Facility Annual Report 2001/2002*, 45 (2002)
- [26] Riley D, Potential for Thomson Scatter With an X-Ray Laser, *IEEE Transactions on Plasma Science*, 31, 1016 (2003)
- [27] Muendel M H, Four-wave frequency conversion of coherent soft x rays in a plasma, *Physical Review A*, 44, 7573 (1991)
- [28] Topping S J, Progress in FWSD non-linear effects with XRLs, *Journal de Physique*, 11, 487 (2001)
- [29] Nabekawa Y, Production of Doubly Charged Helium Ions by Two-Photon Absorption of an Intense Sub-10-fs Soft X-Ray Pulse at 42 eV Photon Energy, *Physical Review Letters*, 94, 043001 (2005)
- [30] Tomassetti G, Two-beam interferometric encoding of photoluminescent gratings in LiF crystals by high-brightness tabletop soft x-ray laser, *Applied Physics Letters*, 85, 4163 (2004)

- [31] Jamelot G, Usefulness of X-ray lasers for science and technology, IEEE Journal of Selected Topics in Quantum Electronics, 5, 1486 (1999)
- [32] Tallents G J, Hot dense plasma opacity measurements using X-ray lasers (2005)
- [33] Linac Coherent Light Source (LCLS) Conceptual Design Report (2002): <http://www-ssrl.slac.stanford.edu/lcls/cdr/>
- [34] The BESSY Soft X-ray Free Electron Laser Technical Design Report (2004): http://www.bessy.de/lab_profile/01.FEL/
- [35] TESLA Technical Design Report (2001): http://tesla.desy.de/new_pages/TDR_CD/
- [36] TESLA Technical Design Report Supplement (2002): http://tesla.desy.de/new_pages/TDR_CD/
- [37] LCLS THE FIRST EXPERIMENTS (2000): <http://www-ssrl.slac.stanford.edu/lcls/science.html>
- [38] Visions of Science: The BESSY SASE-FEL in Berlin-Adlershof (2001): http://www.bessy.de/lab_profile/01.FEL/
- [39] The Science Case for 4GLS (2001): <http://www.4gls.ac.uk/>
- [40] Proposal to the National Science Foundation for a Conceptual Design Study: X-ray Laser User Facility at Bates Laboratory (2003): <http://filburt.lns.mit.edu/xfel/>